X-ray photoelectron-diffraction analysis of oxygen chemisorption on the GaAs(110) surface

D. H. Lee,* J. Chung, and S.-J. Oh†
Department of Physics, Seoul National University, Seoul 151-742, Korea
(Received 20 November 1995)

The initial stage of oxidation on the GaAs(110) surface has been investigated by x-ray photoelectron-diffraction (XPD) analysis, especially paying attention to the XPD pattern of the chemically shifted As component. From the facts that both the As $2p$ and the As $3d$ oxide peak intensities grow as approximately $1/\cos\theta$ when the polar angle θ approaches the glancing emission geometry and that the bulk XPD pattern changes little with the oxygen uptake, it is concluded that the initial oxidation occurs only at the surface and that subsurface oxidation does not take place. The angular variation of the intensity ratio between the oxide and the bulk components of the As core levels clearly shows one specific bonding unit which corresponds to the double bonding of oxygen atoms with As atoms in the direction of 55°–60° relative to the surface normal in the twofold symmetry plane. For other directions, the oxide intensities were shown to be almost uniform, implying that no other dominant bonding units exist.

I. INTRODUCTION

The mechanism of oxygen chemisorption and the oxide layer formation of the GaAs(110) surface has been a controversial problem for the last two decades.[1–16] Because of the very low sticking coefficient of oxygen, it is difficult to form stable, thick oxide layers on a GaAs(110) surface although recent papers report that oxygen chemisorption is increased by several orders of magnitude as a result of illumination with photons at low temperatures below 50 K.[1–3] Despite a large number of theoretical and experimental studies with various techniques [photoemission,[1–7] electron energy loss spectroscopy (EELS),[8] scanning tunneling microscopy (STM),[9,10] etc.] devoted to this subject, several principal problems remain controversial. Unlike the Si(100) or the Si(111) cases in which various oxide phases (Si^{1+},Si^{2+}, Si^{3+}, Si^{4+}) apparently evolve,[17–20] photoemission studies of the GaAs(110) surface seem to show only one dominant oxide phase, which gives a core level chemical shift of about 3 eV to the higher binding energy side for As and 1 eV for Ga compared with the bulk GaAs,[4] and there is a dramatic decrease in the sticking coefficient as the coverage approaches approximately one monolayer (ML).[7,11] Those observations can be well understood with the assumptions that the oxide grows layer by layer and that the first layer has one specific chemisorption geometry. However, low energy electron diffraction (LEED) patterns for this system have shown rather disordered characteristics with an increase in background intensity and the disappearance of features due to surface reconstruction, implying that there does not exist any long-range order for chemisorption sites.[11,12]

From the result of *ab initio* cluster calculations[13,14] for both clean and oxide surfaces, Barton *et al.* suggested a model in which the oxygen atom is doubly bonded to the As atom. For the clean surface reconstruction, their calculation showed very good agreement with the results of dynamical low energy electron diffraction[21,22] and other theoretical calculations[23] where the As atom moves up slightly and the Ga atom moves down from their bulk positions with a tilt angle of about 27°. For the oxygen chemisorption state, they suggested that oxygen atoms are bonded to As atoms with an angle of 56° to the surface normal and with a bond length of 1.63 Å which corresponds to a double bond (As=O) and which is much shorter than the 1.80 Å typical of an As-O single bond. They also predicted the chemical shifts of the As $3d$ and the Ga $3d$ core levels to be 2.6 eV and 0.8 eV, where the Ga shift is caused by only secondary charge transfer. Extended x-ray absorption fine structure (EXAFS) experiments supported this model by providing a 1.5 Å bond length between the As and the O atoms.[24]

A systematic photoemission experiment was performed by Su *et al.*[5] Based on an analysis of the valence band photoemission spectra, they proposed a model similar to Barton *et al.* By comparing the experimental density of valence states (DOVS) of O-GaAs(110), Ga_2O_3, As_2O_3, and O-sputtered GaAs(110), they proposed that at very low coverage below 0.02 ML, Ga-O-Ga units are formed at defect sites and may act as a catalysis to dissociate O_2 molecules into oxygen atoms, and that at intermediate coverage below 1 ML, two specific bonding units of the nonbridging (As=O) and the bridging (Ga-O-As) types are formed as shown in Fig. 1; the latter is absent in Barton *et al.*'s model but is presumed from earlier LEED patterns for n-type GaAs.[11] A few years, often the work of Su *et al.*, an alternative inter-

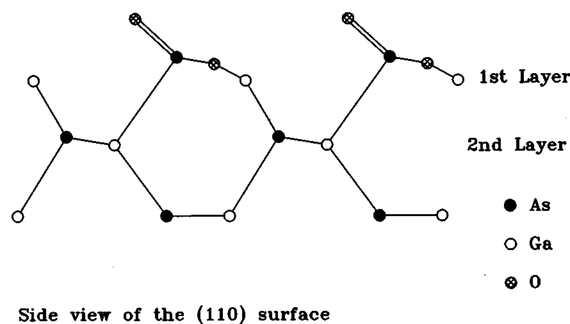

FIG. 1. Su *et al.*'s model for oxygen chemisorption on GaAs(110) surfaces (Ref. 5).

0163-1829/96/53(19)/13038(9)/$10.00 © 1996 The American Physical Society

pretation was proposed by Landgren *et al.*[15] They obtained $3d$ core spectra with very high resolution and fitted them in a manner quite different from those of previous works.[4,11] From their fitting results, they maintained that the oxide grows with various phases for both the As and the Ga atoms as in the Si(100) case and concluded that oxidation about 15 Å into the subsurface takes place from the fact that the oxide component ratio is not much different for both surface-sensitive and bulk-sensitive photon energies. This work stimulated later, more careful investigations of this system. Bertness *et al.* gave their modified interpretation from Su *et al.*'s model.[7] They also fitted the As $3d$ and the Ga $3d$ peaks with several oxide components (0.26, 1.1, 2.6, and 3.0 eV for As and 0.9 eV for Ga) and attributed the large peak shifts to atoms directly bonded with oxygen and the small peak shifts to structural relaxation or secondary charge transfer. As a bonding model, they accommodated the O=As-O-Ga structure put forth by Su *et al*. They also carried out an analysis of the depth distribution of the oxide components for each layer considering the escape depth variation and concluded that oxygen was present only in the first and at most the second atomic layers, in direct contradiction to Landgen *et al.*'s conclusion for subsurface oxide formation.

Though the work of Bertness *et al.* seems to be the most comprehensive so far, it still has some ambiguities with respect to prior works based on photoemission. For example, all the works mentioned above are based on chemical component curve fittings, and the chemisorption models are deduced *indirectly* from these curve-fitting results. There has been no direct evidence as to whether a few specific oxide units really exist or more random phases are mixed in. In that sense, a scanning tunneling microscopy study would be quite helpful. Indeed, one STM study on the O-GaAs(110) surface[10] seems to suggest a quite different picture from that of the above models. The STM images of p-GaAs were taken when the oxygen coverage was only 0.001 ML, and the oxygen atoms seem to lie at the central positions of the Ga-As-Ga triangles with a 2.3 Å lateral distance from the As atom. This implies that each oxygen atom is partially bonded to two Ga atoms and singly bonded to an As atom, which is quite different from the result of Su *et al.*'s model. However, it seems quite unlikely that this is the dominant bonding unit for the intermediate stage of about 1 ML oxygen coverage because the chemical shift of that unit should be much smaller than the dominant 3.1 eV shift for As $3d$ observed by photoemission. Furthermore, the real core position might be somewhat different from the maximum tunneling current position due to polarization of the oxygen atom. Nevertheless, these STM images have directly shown that oxygen is chemisorbed on the nondefect normal site as a dissociated atomic state, even in the very initial stage, and that there exists a different phase from those generally proposed by photoemission studies.

In this paper, we use an angular dependence analysis of x-ray photoelectron spectroscopy (XPS) core level intensities to observe the specific bonding geometry in the oxygen chemisorbed GaAs(110) surface. The XPS peak intensity of a core level from a single crystal generally shows a large angular variation along both the polar and the azimuthal takeoff angles. This is known to be caused by the diffraction of outgoing photoelectrons by neighboring atoms, the so-called x-ray photoelectron-diffraction (XPD) effect.[25,26] Since the XPD process mainly consists of electrons scattering from neighboring atoms, an XPD pattern is available even in the absence of the long-range order which is necessary for LEED studies. Furthermore, the scattering amplitude falls off as $(kR)^{-n}$ for the nth scattering, where k is the wave vector of the outgoing electron and R is the distance between adjacent scatterers. Therefore the diffraction of electrons with energies higher than 500 eV ($kR \gg 1$) can usually be analyzed without serious error by considering only single scattering. In addition, the scattered electron waves in this high energy range are strongly peaked in the forward direction, so an intuitive understanding of the diffraction peak is often possible. One drawback of using high kinetic energy photoelectrons is their rather large inelastic mean free path (typically 20 Å for a kinetic energy of 1000 eV), which makes XPD less surface sensitive. However, if we use the chemically shifted core level peaks from the surface or the adsorbed atoms, the variations of these *chemically shifted component* intensities will give direct information about the positions of the surface or the adatoms, as has been demonstrated recently in several cases.[27]

In this work, we first performed the azimuthal and polar scans of XPS experiments on clean GaAs(110) surfaces obtained by cleavage in an ultra-high vacuum (UHV) chamber; then we compared the results with those calculated using the single scattering cluster (SSC) model. This was mainly to check the experimental setup and how well the SSC model calculation works in the GaAs case. Next, for the main purpose of this work, we performed the azimuthal and polar scans of XPS experiments on oxygen-exposed surfaces and obtained the angular variations of the intensity ratios of the *oxide* component to the bulk GaAs component for a few fixed azimuthal and polar angles. Then these results were compared with those of the SSC model calculations to draw conclusions about the oxygen-bonding geometry.

II. EXPERIMENT

All the XPS spectra were collected using an ESCA/AUGER system manufactured by VSW Scientific Instruments in England. The Al $K\alpha$ ($h\nu = 1486.6$ eV) line was used as the photon source, and a concentric hemispherical analyzer with a multichannel detector was used to measure the photoemitted electron energy distribution with pass energies of 22 eV and 44 eV. The high pass energies were used to increase the intensity rather than to get a higher resolution.

With the angle between the incident x-ray direction and the detected electron direction fixed at 60°, the sample was rotated about the azimuthal and the polar axes for takeoff angle scanning. The polar rotation was made by a direct rotation of the sample manipulator axis. For the azimuthal rotation, special gears were made around the sample holder and were connected to the axis of the outside rotator. The angular resolution of the rotator was $\Delta\theta \sim 0.1°$ for polar scans and $\Delta\phi \sim 0.5°$ for azimuthal scans, where backlash of the gears gave somewhat larger value. The acceptance angle of the electron analyzer was less than 3° based on an estimation of the entrance aperture radius and the distance from the sample.

The sample used in this experiment was Si-doped

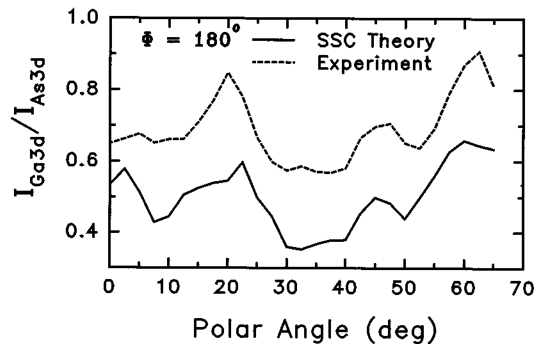

FIG. 2. Polar XPD patterns of the Ga 3d to As 3d intensity ratio at an azimuthal angle of 180°. The y axis for the experimental curve shows the measured ratio of the peak areas. The units of the SSC calculation are arbitrary. This is the same for Figs. 3 and 4.

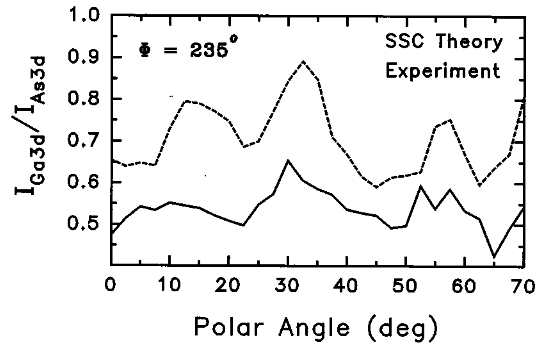

FIG. 3. Polar XPD patterns of the Ga 3d to As 3d intensity ratio at an azimuthal angle of 235°.

n-GaAs with a doping concentration of $(4-6)\times10^{18}$ cm^{-3}. Clean GaAs(110) surfaces were obtained by cleaving a rectangular bar with a cross section of 3×5 mm^2 in an ultrahigh vacuum better than 5×10^{-9} mbar. The sample cleanliness was checked not only with the C 1s and the O 1s XPS spectra, but also with the valence band ultraviolet photoemission (UPS) spectra obtained using He I ($h\nu$= 21.2 eV) and He II ($h\nu$= 40.8 eV) sources. We found that even when C 1s peak appeared to be small in the XPS spectra, the UPS valence-band spectra often showed an appreciable hydrocarbon peak with a binding energy of 7–8 eV. In such a case, the sample was cleaved again. The oxide layer was grown by exposing a clean GaAs(110) surface to pure oxygen gas in a sample preparation chamber. The ion gauge was off during the oxygen exposure to prevent uptake enhancement by the photoexcited oxygen molecules. Many cleaves and oxidations were tried for several samples, but we will only show two oxidation stages of one sample — Si-doped n-type GaAs with a doping concentration of (4–6) $\times10^{18}$ cm^{-3}. The spectra from the other samples were all consistent with the findings reported here. Each oxidation stage was from a different cleave, and the oxygen exposure was 10^{12} L (1 L$=10^{-6}$ torr sec) for the sample surface denoted as $n1$ and 5×10^{12} L for the surface denoted as $n2$.

III. DATA AND RESULTS

A. XPD of a clean GaAs(110) surface

Angular variations of the XPS intensities of clean GaAs surfaces have been reported only for the (100) surface until now,[28–30] so we performed an XPD analysis on a clean (110) surface mainly to check our experimental setup and the SSC calculation. This also gave the reference data for the bulk GaAs, which will be useful not only for our oxygen chemisorption study but also for future studies on the (110) surface because many experiments are performed on this cleavage plane.

The XPD patterns of the polar and azimuthal scans for the Ga 3d to As 3d core level intensity ratio along some fixed direction are shown in Figs. 2, 3, and 4. The reference for the azimuthal angle measurement is marked in Fig. 5. Since it was difficult and usually very inaccurate to evaluate the change of the incident photon flux with the scanning angle, we did not plot the absolute intensity variation for each peak, but only the variation of the intensity ratio between the Ga 3d and As 3d peaks. These curves were generated by taking the photoemission spectra at each angle, which were then curve fitted to get the total area under the peak. The analyzer transmission function was corrected assuming an E^{-1} behavior, and the inelastic background was also subtracted using Shirley's method.[31]

In the same figures, the theoretical predictions from the single scattering cluster (SSC) model are also plotted as solid lines. Over the years, the SSC model has been successfully applied to many adsorbate systems and has proved to be quite a good approximation for most cases.[25,28,32–40] The electron scattering factor $f_j(\theta_j)$ was calculated using Pendry's computer program for LEED analysis[41] with the Herman-Skillman wave functions[42] renormalized as if they

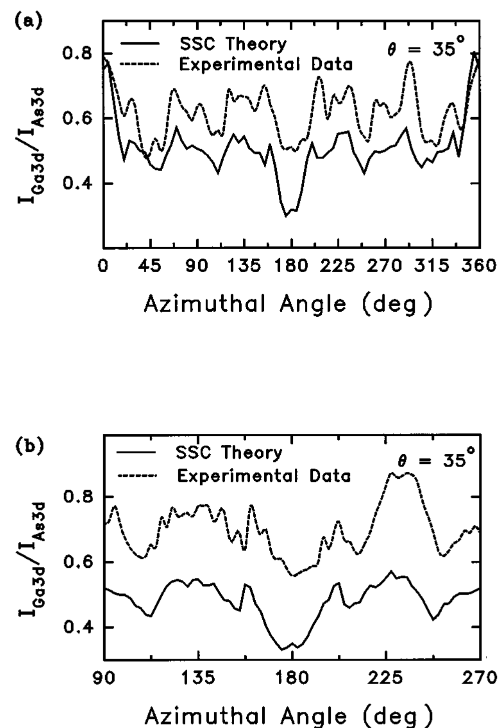

FIG. 4. Azimuthal XPD patterns of the Ga 3d to As 3d intensity ratio at a polar angle of 35°, (a) with an angle increment = 5° and (b) with an angle increment = 2.5° (fine scanning). Some differences are found around 0° and 180°, presumably due to the rapid variation of the intensity with angle.

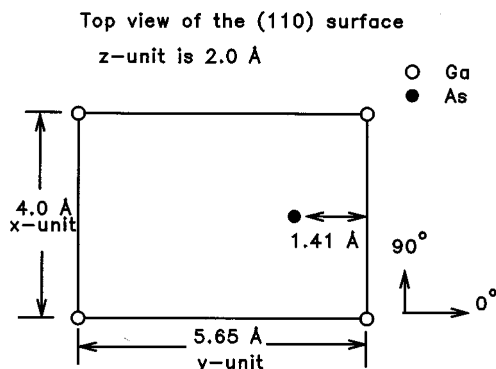

FIG. 5. Top view of the GaAs(110) surface. The angles indicate the reference directions used in the experiment.

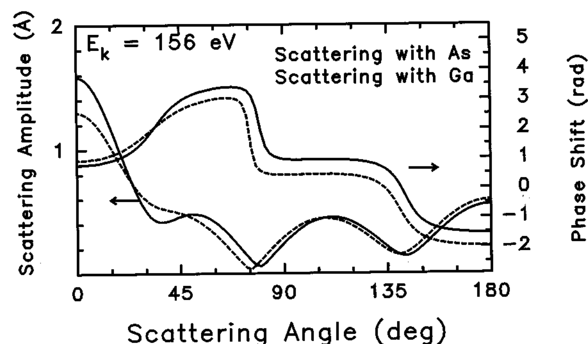

FIG. 7. The calculated scattering amplitudes and the phase shifts for As $2p$ photoelectrons scattered from As atoms and Ga atoms. The kinetic energy of the photoelectron is fixed as $E_{\rm kin} = 156$ eV. No dominant scattering direction is found.

were all within the muffin-tin radius with uniform valence electron wave functions. The resulting scattering factors of the Ga and the As atoms for the photoelectrons from the As $3d$ ($E_k \sim 1440$ eV) and the As $2p$ ($E_k \sim 156$ eV) core levels are shown in Figs. 6 and 7. It can be seen that forward scattering is dominant for the $3d$ peaks; however, this is not the case for the $2p$ peaks which have smaller kinetic energies. Since the scattering factor and the phase shifts depend only on the electron energy and the scattering atom, those for photoelectrons from the Ga $3d$ level ($E_k \sim 1465$ eV) are quite similar to the results for the As $3d$ level. The inelastic mean free path for the attenuation was fixed at 23 Å for both the As $3d$ and the Ga $3d$ levels based on an estimation from the universal equation by Seah and Dench.[43] The surface refraction effect was ignored since the value of the angle change at the surface was estimated to be less than 0.5°, which was much smaller than the angle increments in this experiment. The cluster size used for the SSC simulation was $11\times9\times7$ (the unit for each direction is marked in Fig. 5).

We can see from Figs. 2, 3, and 4 that a very reasonable global coincidence between the experimental XPD patterns and the computer simulation results from SSC calculations is found for both the polar and azimuthal scans. This gives us confidence in our experimental setup and in the SSC calculation. Some discrepancies which can be found in the detailed comparison between the experimental data and the results of SSC calculations may have come from a slight experimental inaccuracy in the angular resolution for the azimuthal scan, because the intensity may vary very rapidly with a small change of angle, as shown in Fig. 4, or they may have come from some arbitrariness in the calculation of scattering factors for fixing the muffin-tin radius and in the assumption that the inelastic effect is isotropic. However, the main discrepancy between the SSC theory and the experiment seems to be caused by the multiple scattering effect. Multiple scattering, in general, need not be considered in high energy electron diffraction, but it has been recently found[40,44,45] that it becomes important in cases where several atoms appear successively along the direction in which the electron propagates. Scattering from successive atoms reduces the XPS intensity significantly because of a ''defocusing'' effect. Since the SSC calculation does not include the defocusing effect, the calculated intensity will be much larger than the experimental intensity for those directions along which multiple scatterings occur. The GaAs structure has no exact one-dimensional chain, but along several directions chainlike arrangements with small positional deviations are found. The ''defocusing'' effect is expected along these directions, and it has been confirmed by the experimental XPD intensity variation of the plasmon loss peak for this GaAs(110) surface[46] in the same manner as for the Al metal case reported earlier.[40,45]

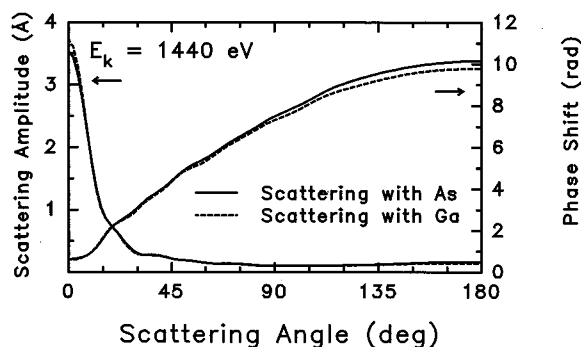

FIG. 6. The calculated scattering amplitudes and the phase shifts for As $3d$ photoelectrons scattered from As atoms and Ga atoms. The kinetic energy of the photoelectron is fixed as $E_{\rm kin} = 1440$ eV. Strong forward scattering is observed.

B. Coverage estimation of an oxygen chemisorbed surface

The saturation of oxygen uptake at about 1 ML coverage may be the most widely accepted property about GaAs(110) oxidation.[7] In this work, almost saturated surfaces with oxygen exposures of 10^{12} L ($n1$) and 5×10^{12} L ($n2$) were studied.

The oxide-state spectra of the Ga and the As $2p$ and $3d$ peaks with their fitting curves are shown in Figs. 8(a)–8(d), and the fitting parameters are given in Table I. Since we are interested in the dominant bonding unit between the oxygen and the Ga or As atoms, the oxide components were fitted as having only one dominant chemically shifted peak for both the As and the Ga, with the shifted peaks having somewhat broader Gaussian widths than those of the main peaks. In Table I, however, it can be seen that the As oxide peaks of oxidation stage $n2$ exposed to more oxygen (5×10^{12} L)

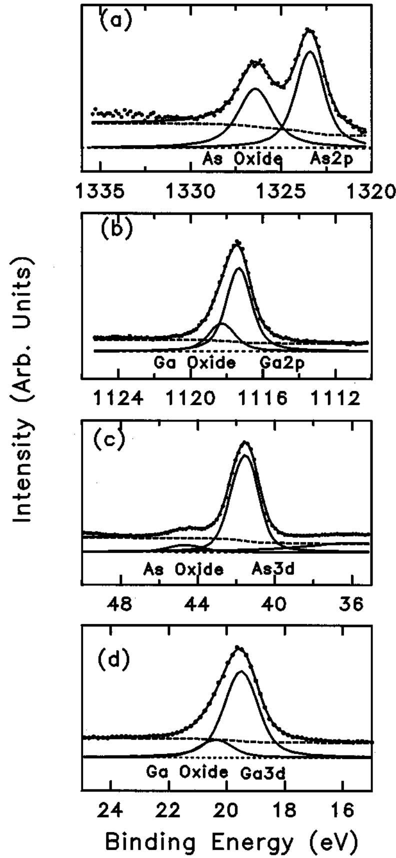

FIG. 8. XPS spectra with their fitting curves at the oxidation stage $n1$ (1×10^{12} L oxygen exposure). The polar takeoff angle is 50° and the azimuthal angle is 180°. (a) As $2p$, (b) Ga $2p$, (c) As $3d$, and (d) Ga $3d$. The small bump at ~36 eV in (c) is the first plasmon loss peak of Ga $3d$.

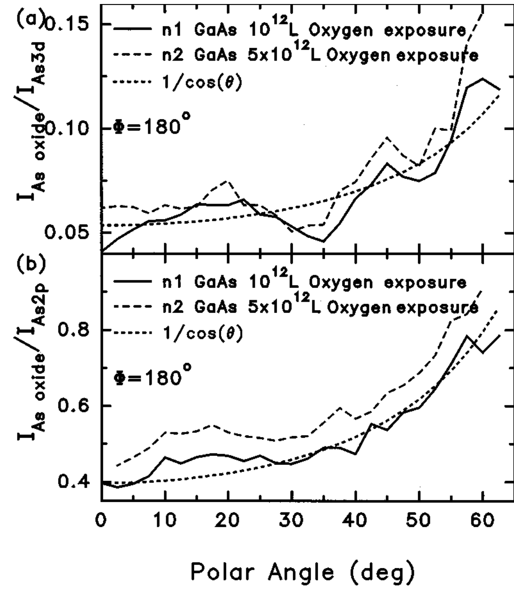

FIG. 9. The polar patterns of the intensity ratio of the oxide component peak relative to the main component peak for the $n1$ (10^{12} L oxygen exposure) and the $n2$ (5×10^{12} L oxygen exposure) oxidation stages for (a) As $3d$ and (b) As $2p$. The azimuthal angle is 180°. In both figures, the oxide intensity ratio variations are almost the same for the two oxygen-exposed surfaces, which ensures the reproducibility of the measurements. The dotted line represents a $1/\cos\theta$ curve.

have slightly larger chemical shifts than those of stage $n1$ with an oxygen exposure of 10^{12} L. This probably implies that components of smaller energy shifts, which are related to the secondary charge-transfer effect, really exist, but their intensity and energy positions will not affect our analysis here.

The oxygen coverage and the penetration depth from the surface can be estimated by analyzing the variation of the intensity ratio between the oxide component peak and the bulk peak either along the polar rotation or with different electron kinetic energies (e.g., As $2p$ and As $3d$). In Fig. 9, the polar scans of the intensity ratio of the oxide peak relative to the bulk peak for the As $3d$ and As $2p$ core levels are shown. In this figure, we can see that both the $2p$ and the $3d$ patterns show little difference for the different cleavages $n1$ and $n2$, ensuring reproducibility. Another important fact is that for both the As $2p$ and $3d$ levels, the oxide intensity ratio closely follows a $1/\cos\theta$ curve, except for the case of As $3d$ in the low θ region where the diffraction effect becomes important as shown below. This fact is consistent with the notion that the oxygen atoms are confined to the surface layer(s) and do not penetrate deeply into the bulk.

Using the following general equation by Seah and Dench[43] for the inelastic mean free path, the oxygen coverage can be roughly estimated:

TABLE I. Results of curve fittings for the As $2p$, the Ga $2p$, and the As $3d$ peaks. Here, IMFP stands for the electron inelastic mean free path estimated by Seah and Dench's relation (Ref. 43) and HWHM stands for the half width at half maximum.

Stage	$n1$ (10^{12} L O_2 exposure)			$n2$ (5×10^{12} L O_2 exposure)		
Atomic level	As $2p$	Ga $2p$	As $3d$	As $2p$	Ga $2p$	As $3d$
Kinetic energy (eV)	158.6	364.5	1440.7	158.6	364.5	1440.7
IMFP (Å)	7.8	11.8	23.4	7.8	11.8	23.4
Lorentzian HWHM (eV)	1.16	1.00	0.55	1.24	0.98	0.55
Gaussian HWHM of main peak (eV)	1.11	1.00	1.02	1.07	0.92	1.02
Gaussian HWHM of oxide peak (eV)	1.56	1.00	1.45	1.52	0.92	1.45
Chemical shift (eV)	2.98	1.00	2.97	3.02	0.95	3.03
I_{oxide}/I_{total} at $\theta=0°$	0.28	0.09		0.31		0.17
Thickness of oxide layer (Å)	2.2			2.4		
No. of bonding atoms per one surface atom	1.1			1.2		

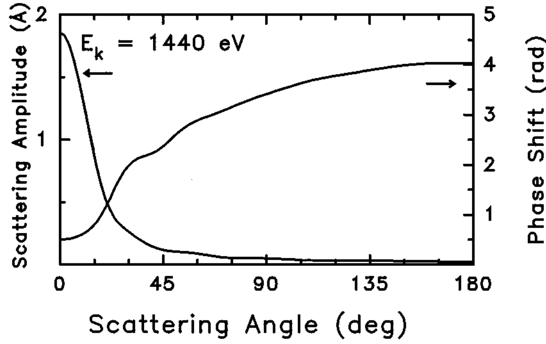

FIG. 10. The scattering amplitude and the phase shift for As $3d$ photoelectrons (E_{kin} = 1440 eV) scattered from oxygen atoms. The forward scattering is weaker than the cases of scattering from As and Ga atoms shown in Fig. 6.

$$\lambda = 0.41\left(\frac{E}{d}\right)^{1/2} (\mathrm{nm})$$

where E is the electron kinetic energy in eV and d is the atomic concentration in nm^{-3}. Assuming there exists no subsurface oxidation, the depth l of oxygen-bonded As atoms can be evaluated from the following equation at $\theta = 0°$:

$$\frac{I_{\mathrm{oxide}}}{I_{\mathrm{As}}} = \frac{\int_{x=O}^{l} \exp(-x/\lambda)dx}{\int_{x=l}^{\infty} \exp(-x/\lambda)dx} = \frac{1-\exp(-l/\lambda)}{\exp(-l/\lambda)}.$$

We evaluated the thickness of oxide layers and the corresponding numbers of bonding oxygen atoms per each surface atom using the above equation, and the results are shown in Table I. From these results, it can be said that one arsenic atom at the topmost layer bonds with approximately one oxygen atom, under the assumption that most of the bonds are at the topmost layer.

C. Bonding structure study by XPD analysis of the oxide component

We next want to see by XPD analysis whether or not a dominant chemisorption unit especially bonded to the As atom exists, and if it does, what the bonding angle and the bond length are. Because of the twofold symmetry of the (110) surface, an oxygen atom doubly bonded to As will exist on the plane of 0° or 180° in the azimuthal angle if a static configuration is assumed. Hence all the polar scan experiments were done at an azimuthal angle of 180°, and the azimuthal scans were done at polar angles of 50° and 56°, which are close to the expected bonding angle proposed by Barton *et al.*'s cluster calculation.[13,14]

In Fig. 10, the scattering amplitude and the phase shift for the scattering of photoelectrons from the As or Ga $3d$ core levels with oxygen atoms are shown. The forward focusing is slightly weaker than those for the scattering from As or Ga atoms shown in Fig. 6. In Fig. 11, the experimental polar XPD patterns of the intensity ratio of the As $3d$ oxide component relative to the bulk As peak along the twofold symmetry plane are shown. Since the photoelectron escape depth is not very short in this kinetic energy range, some of the XPD features come from the bulk As $3d$ intensity variation.

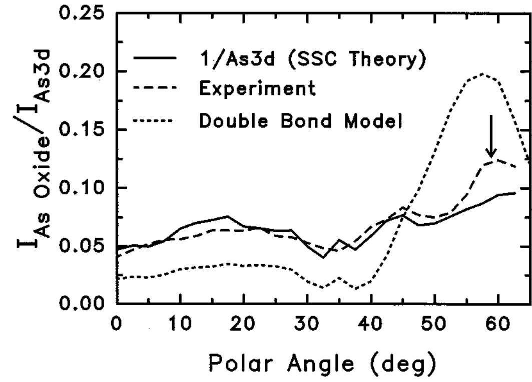

FIG. 11. The polar pattern of the intensity ratio of the As $3d$ oxide component relative to the bulk component for the $n1$ (10^{12} L oxygen exposure) oxidation stage at an azimuthal angle 180° is compared with the calculated patterns of $1/I_{\mathrm{As}\,3d}$ and of the double-bond model. In the experimental pattern, a peaking feature is clearly seen around 55°–60° and is similar to the calculated pattern for the double-bond model.

To separate out this contribution, we show in the same figure, with the solid line, the calculated pattern of $1/I_{\mathrm{bulk\ As}}$, which in effect corresponds to the case of a uniformly oriented oxygen configuration. In global features, the experimental XPD patterns are fairly similar to those of $1/I_{\mathrm{bulkAs}}$, except for a remarkable feature between 55° and 65°. This feature is precisely what is expected from the oxygen-bonding geometry of Barton *et al.*'s model[13,14] due to the forward scattering effect of photoelectrons, as can be seen in the calculation curve for this bonding geometry. It must be noted, though, that the observed intensity peak in this direction is much less than the calculated result for full oxygen coverage.

We can also look at the azimuthal XPD pattern. The experimentally obtained azimuthal patterns with polar angles of 56° and 50° are shown in Fig. 12. In the experimental pattern at $\theta = 56°$, a distinguishable peaking is found around 180°, whereas the calculated pattern for the uniformly oriented oxide case ($1/I_{\mathrm{bulk\ As}}$) shows no dominant peak in that region. The enhancement of the oxide component at 180° can be more directly observed from the comparison of the raw spectra shown in Fig. 13. This feature is also consistent with the double-bonding unit proposed by Barton *et al.* On the other hand, in the scan at a $\theta = 50°$ polar angle, no remarkable feature is found, and the experimental pattern is globally coincident with the $1/I_{\mathrm{bulk\ As}}$ calculation curve. This fact is consistent with the polar experimental pattern in Fig. 11, which shows little deviation from the uniform oxide case at $\theta = 50°$.

We can conclude from the experimental XPD patterns for both the polar angle and the azimuthal angle scans shown above that double bonding with As atoms does exist with a bonding angle of 55°–65°, which is similar to the predicted value of Barton *et al.*'s model, even though its forward peaking intensity is much less than expected from the SSC calculation for full oxygen coverage.

IV. DISCUSSION

We can note a few things from the above XPD study of the oxygen-chemisorbed GaAs (110) surface. First, care

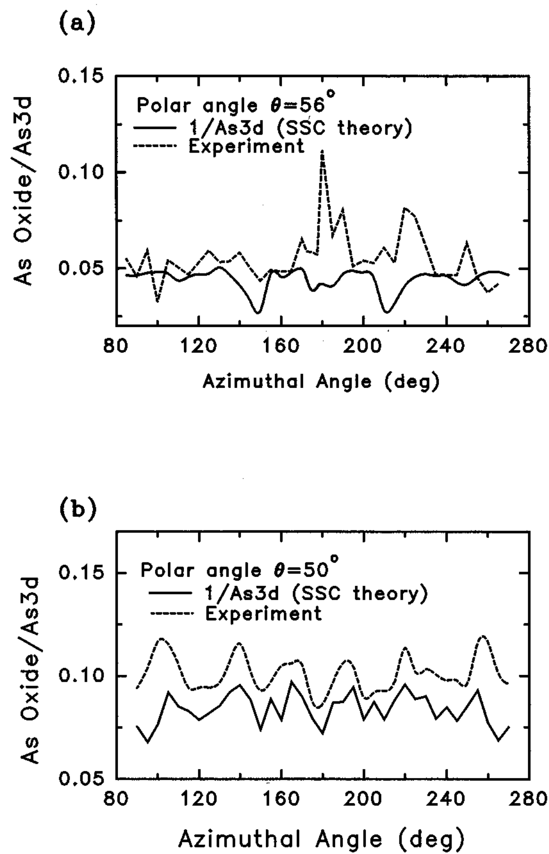

FIG. 12. The azimuthal patterns of the intensity ratios of the As $3d$ oxide component relative to the bulk component for the $n1$ (10^{12} L oxygen exposure) oxidation stage are compared with the calculated azimuthal pattern of $1/I_{\mathrm{As}\,3d}$. The polar angles are (a) $\theta=56°$ and (b) $\theta=50°$. In the $\theta=56°$ experimental XPD pattern, a peaking is clearly found around 180°. This feature is not seen in the calculated result for the uniformly oriented oxide case ($I/I_{\mathrm{bulk\ As}}$). No such feature is found in the experimental pattern of $\theta=50°$.

must be taken in estimating the oxide layer thickness and the variation of the inelastic mean free path (IMFP) with kinetic energy from the measurement of the oxide component ratios, because the bulk intensity itself shows a large variation with the kinetic energy and the photoelectron takeoff angle. According to our data the values of $I_{\mathrm{Ga}\,2p}/I_{\mathrm{As}\,2p}$ for the bulk Ga and As $2p$ peak intensities change as much as 50% with the polar takeoff angle. In this sense, Landgren *et al.*'s result[15] of a larger oxide component ratio than expected at the bulk-sensitive photon energy might be due to the photoelectron diffraction effect. Also, Bertness *et al.*'s evaluation[7] of the IMFP curve with kinetic energy up to 300 eV might have errors since they did not consider the XPD effect at all. For single crystal surfaces, it has been shown[47] that only the average of the intensity ratio over the wide-angle range should be used for an escape depth estimate. Our estimate in Sec. III B has been checked to satisfy this requirement.

We have inferred from the polar angle scans of the oxide component intensities of the As $2p$ and $3d$ peaks that the oxidation is confined to the surface and that the oxygen does not penetrate into the subsurface layers. There is another piece of decisive evidence that subsurface oxidation hardly takes place. If the oxygen atoms penetrated into the bulk, the

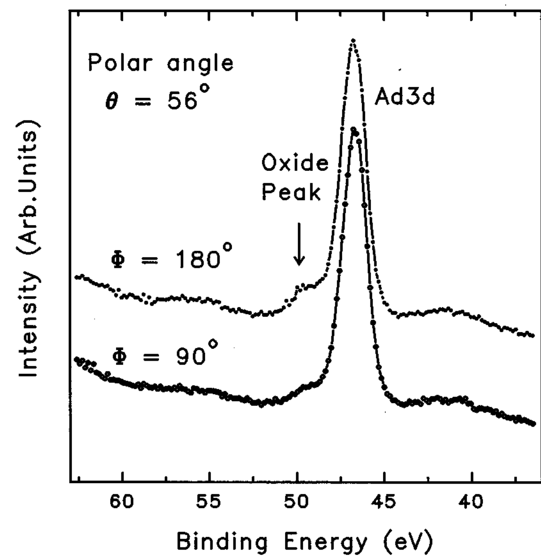

FIG. 13. As $3d$ XPS spectra for a polar angle of 56° but at different azimuthal angles of 90° and 180°. The intensity ratio of the oxide peak to the main bulk peak is distinguishably enhanced at an azimuthal angle of 180°.

XPD pattern of the bulk component would significantly change. However, as shown in Fig. 14, the polar XPD pattern of $I_{\mathrm{Ga}\,3d}/I_{\mathrm{As}\,3d}$ from the oxygen-chemisorbed surface is quite similar to that from the clean surface, which implies that the bulk remains almost unaffected by the oxygen uptake.

With respect to the chemisorption structure, the XPD analysis gave more direct information. A unique feature over the uniform background was found at the polar angle around 55°–65° on the twofold symmetry plane, and was observed in both the polar and the azimuthal patterns. From a comparison with the earlier cluster calculation by Barton *et al.*,[13,14] this feature is presumed to correspond to a mixture of double bonding with arsenic atoms (O=As) and addi-

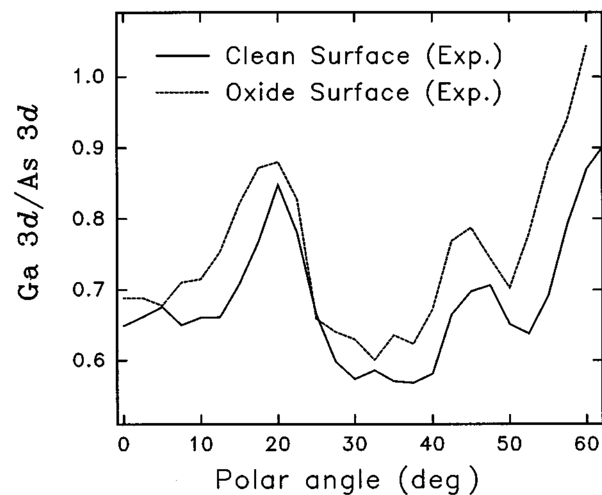

FIG. 14. Polar XPD patterns of the intensity ratio of the Ga $3d$ to the As $3d$ bulk peaks for clean and oxidized surfaces at an azimuthal angle of 180°. These two patterns are substantially the same, implying that oxygen does not disrupt the bulk GaAs structure significantly.

tional bridging bonding (O=As-O-Ga). The fact that the measured intensity variation of this feature is weaker than predicted by the SSC calculation may have several origins. First, the actual scattering factor may be much less forward directional than assumed in the SSC calculation due to the spherical wave character of the photoelectrons. Since the expected bond length is as short as 1.63 Å, the correction for the small atom approximation might reduce the forward peaking by as much as one-half.[26] Next, the irregularity of the bonding, such as the second layer disruption or relaxation due to nearest oxygen bonding with Ga, will increase the intensities for other directions. Another possibility is the rotation of this bonding unit along the azimuthal angle due to the thermal motion, since our measurements were taken at room temperature. It is also possible that the above unit is not a dominant one and that there exist other oxide units. However, this is not very likely because of the fact that no other remarkable features are found in the azimuthal scans of Fig. 12, although only two polar angles, 50° and 56°, may not be sufficient to exclude all possibilities.

V. CONCLUSIONS

The XPS intensity from each element (Ga or As) of the clean (110) surface of the GaAs single crystal shows a large variation with both polar and azimuthal takeoff angles. The SSC model calculations for the photoelectron diffraction effect produce XPD patterns quite similar to the experimental ones. The main discrepancy between the experimental and the SSC calculational results is due to the ''defocusing effect'' along the directions of chainlike arrangements, which can be confirmed by the reduction of the plasmon loss peak intensity at those angles.

The amount of As oxide at the oxygen-saturated coverage was estimated as corresponding to about one oxygen bonding per one arsenic atom at the topmost layer. From the facts that both the As $2p$ and $3d$ oxide ratios approximately follow the $1/\cos(\theta)$ curve and that the bulk XPD pattern changes little with oxygen uptake, it was concluded that the oxygen atoms make bonds only at the surface and that subsurface oxidation does not take place.

By analyzing the angular variation of the intensity ratio of the oxide component to the bulk component, we could make a direct observation of one specific surface bonding unit. In both the polar and the azimuthal scans, a feature presumed to correspond to double bonding with As atoms was clearly observed around a polar angle of 55°–65° in the twofold symmetry plane. For other directions, the oxide intensities were determined to be almost uniform. It seems that no dominant bonding unit exists other than the above double-bonding unit.

ACKNOWLEDGMENT

This work was support by a grant from the Korean Science and Engineering Foundation, KOSEF 91-0100-07013.

*Present address: Samsung Electronics Semiconductor Business, R&D Center, Basic Research Team, P.O. Box 37, Suwon, Korea.

†Author to whom all correspondence should be addressed.

[1] D. J. Frankel, Y. Yukun, R. Avci, and G. P. Lapeyre, J. Vac. Sci. Technol. A **1**, 679 (1983).

[2] K. Stiles, D. Mao, and A. Kahn, J. Vac. Sci. Technol. B **6**, 1170 (1988).

[3] J. M. Seo, S. G. Anderson, T. Komeda, C. Capasso, and J. H. Weaver, Phys. Rev. B **41**, 5455 (1990).

[4] P. Pianetta, I. Lindau, C. Garner, and W. E. Spicer, Phys. Rev. Lett. **35**, 1356 (1975); **37**, 1356 (1976).

[5] C. Y. Su, I. Lindau, P. W. Chye, P. R. Skeath, and W. E. Spicer, Phys. Rev. B **25**, 4045 (1982).

[6] T. Miller and T.-C. Chiang, Phys. Rev. B **29**, 7034 (1984).

[7] K. A. Bertness, J.-J. Yeh, D. J. Friedman, P. H. Mahowald, A. K. Wahi, T. Kendelewicz, I. Lindau, and W. E. Spicer, Phys. Rev. B **38**, 5406 (1988).

[8] F. Bartels and W. Mönch, Surf. Sci. **143**, 315 (1984).

[9] J. A. Stroscio, R. M. Feenstra, and A. P. Fein, Phys. Rev. Lett. **58**, 1668 (1987).

[10] J. A. Stroscio, R. M. Feenstra, and A. P. Fein, Phys. Rev. B **36**, 7718 (1987).

[11] R. Dorn, H. Lüth, and G. J. Russel, Phys. Rev. B **10**, 5049 (1974).

[12] A. Kahn, D. Kanani, P. Mark, P. W. Chye, C. Y. Su, I. Lindau, and W. E. Spicer, Surf. Sci. **87**, 325 (1979).

[13] J. J. Barton, W. A. Goddard III, and T. C. McGill, J. Vac. Sci. Technol. **16**, 1178 (1979).

[14] J. J. Barton, C. A. Swarts, W. A. Goddard III, and T. C. McGill, J. Vac. Sci. Technol. **17**, 164 (1980).

[15] G. Landgren, R. Ludeke, Y. Jugnet, J. F. Morar, and F. J. Himpsel, J. Vac. Sci. Technol. B **2**, 351 (1984); Phys. Rev. B **30**, 4839 (1984).

[16] E. J. Mele and J. D. Joannopoulos, Phys. Rev. B **18**, 6999 (1978).

[17] F. J. Grunthaner, P. J. Grunthaner, R. P. Vasquez, B. F. Lewis, J. Maserjian, and A. Madhukar, Phys. Rev. Lett. **43**, 1683 (1979).

[18] G. Hollinger and F. J. Himpsel, Phys. Rev. B **28**, 3651 (1983).

[19] F. J. Himpsel, F. R. McFeely, A. Taleb-Ibrahimi, J. A. Yarmoff, and G. Hallinger, Phys. Rev. B **38**, 6084 (1988).

[20] V. D. Borman, E. P. Gusev, Yu. Yu. Lebedinskii, and V. I. Troyan, Phys. Rev. Lett. **67**, 2387 (1991).

[21] R. J. Meyer, C. B. Duke, A. Paton, A. Kahn, E. So, J. L. Yeh, and P. Mark, Phys. Rev. B **19**, 5194 (1979).

[22] S. Y. Tong, and W. N. Mei, J. Vac. Sci. Technol. B **2**, 393 (1984).

[23] D. J. Chadi, Phys. Rev. Lett. **41**, 1062 (1978); Phys. Rev. B **19**, 2074 (1979).

[24] J. Stöhr, R. S. Bauer, J. C. McMenamin, L. I. Johansson, and S. Brennan, J. Vac. Sci. Technol. **16**, 1195 (1979).

[25] C. S. Fadley, Prog. Surf. Sci. **16**, 275 (1984); D. J. Friedman and C. S. Fadley, J. Electron Spectrosc. Relat. Phenom. **51**, 689 (1990); C. S Fadley, in *Synchrotron Radiation Research: Advances in Surface Science*, edited by R. Z. Bachrach (Plenum, New York, 1992), Chap. 11.

[26] S. A. Chambers, Adv. Phys. **40**, 357 (1991); Surf. Sci. Rep. **16**, 293 (1992).

[27] E. L. Bullock, R. Gunnella, L. Patthey, T. Abukawa, S. Kono, C. R. Natoli, and L. S. O. Johansson, Phys. Rev. Lett. **74**, 2756 (1995).

[28] S. A. Chambers, Phys. Rev. B **42**, 10 865 (1990).

[29] P. Alnot, F. Wyczisk, and A. Friederich, Surf. Sci. **162**, 708 (1985).

[30] S. Evans, and M. D. Scott, Surf. Interface Anal. **3**, 269 (1981).

[31] D. A. Shirley, Phys. Rev. B **5**, 4709 (1972).

[32] S. Kono, S. M. Goldberg, N. F. T. Hall, and C. S. Fadley, Phys. Rev. Lett. **41**, 1831 (1978); Phys. Rev. B **22**, 6085 (1980).

[33] L.-G. Petersson, S. Kono, N. F. T. Hall, C. S. Fadley, and J. B. Pendry, Phys. Rev. Lett. **42**, 1545 (1979).

[34] P. J. Orders, R. E. Connelly, N. F. T. Hall, and C. S. Fadley, Phys. Rev. B **24**, 6163 (1981).

[35] E. L. Bullock and C. S. Fadley, Phys. Rev. B **31**, 1212 (1985).

[36] D. A. Wesner, F. P. Coenen, and H. P. Bonzel, Phys. Rev. Lett. **60**, 1045 (1988).

[37] R. S. Saiki, G. S. Herman, M. Yamada, J. Osterwalder, and C. S. Fadley, Phys. Rev. Lett. **63**, 283 (1989).

[38] S. A. Chambers and V. A. Loebs, Phys. Rev. Lett. **63**, 640 (1989).

[39] R. Baptist, S. Ferrer, G. Grenet, and H. C. Poon, Phys. Rev. Lett. **64**, 311 (1990).

[40] J. Osterwalder, T. Greber, S. Hüfner, and L. Schlapbach, Phys. Rev. B **41**, 12 495 (1990).

[41] J. B. Pendry, *Low Energy Electron Diffraction* (Academic Press, London, 1974).

[42] F. Herman and S. Skillman, *Atomic Structure Calculation* (Prentice-Hall, Englewood Cliffs, NJ, 1963).

[43] M. P. Seah and D. P. Dench, Surf. Interface Anal. **1**, 2 (1979).

[44] M.-L. Xu, J. J. Barton, and M. A. Van Hove, Phys. Rev. B **39**, 8275 (1989).

[45] G. S. Herman and C. S. Fadley, Phys. Rev. B **43**, 6792 (1991).

[46] D. H. Lee, J. Chung, and S.-J. Oh, J. Korean Vac. Soc. **2**, 171 (1993).

[47] L. S. O. Johansson, R. Gunnella, E. L. Bullock, C. R. Nattoli, and R. I. G. Uhrberg (unpublished).